Magnitude and Location of Surface Charges on *Myxicola* Giant Axons

TED BEGENISICH

From the Department of Biophysics, University of Maryland School of Medicine, Baltimore, Maryland 21201. Dr. Begenisich's present address is the Department of Physiology and Biophysics, University of Washington School of Medicine, Seattle, Washington 98195.

ABSTRACT The effects of changes in the concentration of calcium in solutions bathing *Myxicola* giant axons on the voltage dependence of sodium and potassium conductance and on the instantaneous sodium and potassium current-voltage relations have been measured. The sodium conductance-voltage relation is shifted along the voltage axis by 13 mV in the hyperpolarizing direction for a fourfold decrease in calcium concentration. The potassium conductance-voltage relation is shifted only half as much as that for sodium. There is no effect on the shape of the sodium and potassium instantaneous current-voltage curves: the normal constant-field rectification of potassium currents is maintained and the normal linear relationship of sodium currents is maintained. Considering that shifts in conductances would reflect the presence of surface charges near the gating machinery and that shape changes of instantaneous current-voltage curves would reflect the presence of surface charges near the ionic pores, these results indicate a negative surface charge density of about 1 electronic charge per 120 A^2 near the sodium gating machinery, about 1 e/300 A^2 for the potassium gating machinery, and much less surface charge near the sodium or potassium pores. There may be some specific binding of calcium to these surface charges with an upper limit on the binding constant of about 0.2 M^{-1}. The differences in surface charge density suggest a spatial separation for these four membrane components.

INTRODUCTION

Frankenhaeuser and Hodgkin (1957) showed that changes in the external calcium concentration translated the relationship between membrane conductance and potential along the voltage axis. They attributed this effect to changes in the potential across the membrane resulting from an interaction between calcium and fixed charges on the external membrane surface. In the years since this pioneering work, there have been a number of other observations of the effects of changes in the concentration of external divalent cations (particularly calcium) on voltage clamped nerve fibers (for example: Hille, 1968; Rojas and Atwater, 1968; Blaustein and Goldman, 1968, Gilbert and

Ehrenstein, 1969; Mozhayeva and Naumov, 1970; Brismar, 1973). These effects have generally been attributed to an uncovering of membrane fixed surface charges when the external divalent cation concentration is reduced. An alternate explanation is that calcium ions block sodium current in a voltage-dependent manner (Goldman, 1964; Fishman et al., 1971; Moore and Jakobsson, 1971). A major difficulty with this blocking hypothesis is the observation of voltage shifts with changes only in the concentration of monovalent ions (Chandler et al., 1965; Mozhayeva and Naumov, 1970; Brismar, 1973; Hille et al., 1974). This paper tests the proposition that the voltage shifts of ionic conductances are explained by the presence of fixed charges on the membrane surface. A question that is still unanswered is whether these charges are diffusely distributed over the entire membrane surface or locally concentrated near the membrane constituents underlying excitation (or both). The experiments to be described here were designed to determine the surface charge densities in the vicinity of the sodium and potassium conductance regulating mechanisms, the "voltage sensors," and compare these with the surface charge densities near the sodium and potassium permeation sites, the pores.

METHODS

The experiments described here were performed on the giant axon of the marine worm *Myxicola infundibulum*. The dissection of this preparation is described in detail by Binstock and Goldman (1969). The mean values of the resting potential and diameter of axons used in this study were −61.7 mV (range −55 to −66 mV) and 501 μm (range 425–625 μm), respectively. The average value of the action potential was 114 mV with only one axon with a value below 110 mV.

The chamber, temperature control system, and the voltage-clamp circuit have been previously described (Begenisich and Lynch, 1974). The temperature was maintained at 5°C for all experiments, except the instantaneous sodium current-voltage experiments where a temperature of 2°C was used.

Series resistance compensation was used throughout. The series resistance, R_s, was measured from the jump in the membrane potential produced by a brief constant current pulse. I find an average value of R_s of 10 Ω-cm². This is in good agreement with the value of about 13 Ω-cm² found by Goldman and Schauf (1972). The R_s compensation was increased to the point of ringing of the potential trace. I find, as did Goldman and Schauf (1972), that about two-thirds of the measured R_s was actually compensated for by this technique. The effects of the uncompensated series resistance are discussed in the next section.

The external electrode was a saturated KCl, agar bridge connected to the external voltage preamplifier via a Ag/AgCl wire. The internal electrode was of the "piggy-back" arrangement (Chandler and Meves, 1965), with the current delivered via a 50-μm platinum black (10% Ir) wire. The voltage electrode was a glass pipette 75 μm at the tip, containing a solution of 0.56 M KCl; a Ag/AgCl wire connected the KCl solution to the internal voltage preamplifier. A 25-μm unplatinized Pt (10%

Ir) wire inserted into the shank of the pipette was used to reduce the high frequency impedance.

There is, in general, a liquid junction potential between the KCl solution of the internal pipette and the *Myxicola* axoplasm. Cole and Moore (1960) have shown that for squid axoplasm this value is 10–12 mV for a 0.5 M KCl electrode. Binstock and Goldman (1971) have demonstrated that a similar value is appropriate for *Myxicola.* Therefore, the membrane potential, V, is reported corrected for a liquid junction potential of 10 mV.

The peak values of sodium current, I_{Na}, were obtained by subtracting the leakage and potassium current components obtained by repeating each voltage-clamp sequence in the appropriate solution containing 10^{-6} M tetrodotoxin (TTX). Potassium currents, I_K, were measured in the presence of TTX and corrected for leakage currents, I_L. A small (usually 30 mV) depolarizing step was made and the current minimum taken as the leakage current. This value was then scaled linearly to provide leakage corrections at other voltages.

Instantaneous sodium currents, I'_{Na}, were measured at the time of peak sodium currents. The measurement of this current is difficult because of its very fast time-course and its contamination with capacitative current, I_C. The experiments on instantaneous sodium currents were done at 2°C where the kinetics are slower.

The sodium tail currents were extrapolated back to their instantaneous or zero time values by first subtracting $I_L + I_C + I_K$ (from the same solution containing TTX) at different times after the step and then plotting the log of these tail values as a linear function of time. The tails are initially close to exponential and the straight line on the semilog plot can easily be extrapolated to the value at zero time.

The potassium instantaneous currents were measured during the "steady-state" phase of membrane current (in the presence of TTX), and the resulting current corrected for I_L and I_C. This correction was made by using a mirror image of the pulse sequence. That is, for every depolarizing prepulse and test pulse sequence, a pre- and test pulse of the same amplitude but opposite in sign was used. The currents obtained from the test pulses and their mirror images were added to yield uncontaminated potassium instantaneous currents. The time-course of the potassium tails is much slower than that of sodium and the measurement of the instantaneous value, to be called I'_K, is much less sensitive to the time at which the measurement was made, and the extrapolation back to zero time can be done without resorting to semilog plots.

Sodium and potassium conductance (g_{Na} and g_K) are defined in the following ways:

$$g_{Na} = I_{Na}/(V - V_{Na}),$$
$$g_K = I_K/(V - V_K),$$

where I_{Na} is the sodium current (measured at its peak), V is the membrane voltage when the measurement is made, and V_{Na} is the reversal potential for the sodium current. (The potassium parameters are defined analogously.)

The artificial seawater (ASW) solutions used in this study are shown in Table I. A constant osmolarity was maintained as $CaCl_2$ was added by reducing the concentration of sucrose. Table I shows the measured osmolarity of the Ca ASW solutions

TABLE I
ARTIFICIAL SEAWATER SOLUTIONS

Salt	ASW	5 Ca^{++} ASW	10 Ca^{++} ASW	25 Ca^{++} ASW	50 Ca^{++} ASW	100 Ca^{++} ASW
	mM	*mM*	*mM*	*mM*	*mM*	*mM*
NaCl	430	370	370	370	370	370
KCl	10	10	10	10	10	10
$CaCl_2$	10	5	10	25	50	100
$MgCl_2$	50	0	0	0	0	0
Sucrose	0	232	220	185	127	10
HEPES	1	1	1	1	1	1
Relative osmolarity	1.0	0.98	0.98	0.98	0.99	0.98

with respect to the value of ASW. Note that the NaCl concentration (370 mM) in the calcium solutions is less than that of normal ASW. This was necessary to prevent the 100 Ca^{++} ASW solution from being hyperosmotic. Note also that Ca^{++} is the only divalent cation used in the Ca ASW solutions. All solutions were buffered to a room temperature (21°C) pH of 7.4 with 1 mM HEPES (*N*-2-hydroxyethylpiperazine-*N'*-2-ethanesulfonic acid). The pK_a of HEPES has a rather small temperature coefficient (−0.014/°C) and the pH at 5° is therefore about 7.6.

The data in this work are analyzed by surface potential theory according to the Grahame equation (Grahame, 1947) modified to include specific calcium binding:

$$\sigma_d^2 = \frac{kT\epsilon}{2\pi} \sum n_i \left[\exp\left(-Z_i e\psi_0/kT\right) - 1\right]$$
$$\sigma_d = \sigma_T/[1 + K[\mathrm{Ca}] \exp\left(-2e\psi_0/kT\right)] \quad (1)$$

σ_d is the apparent surface charge density in the presence of calcium binding to negative sites, X^-, according to the scheme $Ca^{++} + X^- \leftrightarrow CaX$ with K the equilibrium binding constant (M^{-1}). σ_T is the surface charge density if there were no calcium binding ($K = 0$). n_i is the bulk concentration of the ith ionic species, and Z_i is the valence. ψ_0 is the surface potential and ϵ the dielectric constant of the aqueous solution. k, T, and e are, respectively, Boltzmann's constant, the absolute temperature, and the charge of an electron.

The foundation for this analysis is described by Gilbert and Ehrenstein (1969) and McLaughlin et al. (1971). Davies and Rideal (1963) and Aveyard and Haydon (1973) have discussed the approximations made in the development of the theory and McLaughlin et al. (1971) have discussed its applicability to biological membranes.

Absolute values of the surface potential, ψ_0, are not measured here, rather changes in the surface potential from a standard solution (100 mM Ca ASW) to a test solution are measured. Eq. 1 is solved numerically (Newton-Raphson iteration technique) for the two calcium concentrations with various combinations of surface charge density σ_T, and binding constant K, until the best fit to the observed change in surface potential is obtained. It should be emphasized that the prameters σ_T and

K derived in this manner are average values for only the region of the membrane under study (e.g. the region of the sodium voltage sensor), not for the membrane surface as a whole.

RESULTS

External Calcium and Sodium Conductance

Fig. 1 shows the sodium conductance, g_{Na}, V relations in 100 and 10 mM Ca^{++}-containing solutions. At negative values of V the relations for both 10 and 100 mM Ca^{++} rise rather linearly on this semi-log plot and with about the same slope. The potential at which the conductance reaches one-half of the saturation value, $V_{1/2}$, is recorded and the change in this value from the 100

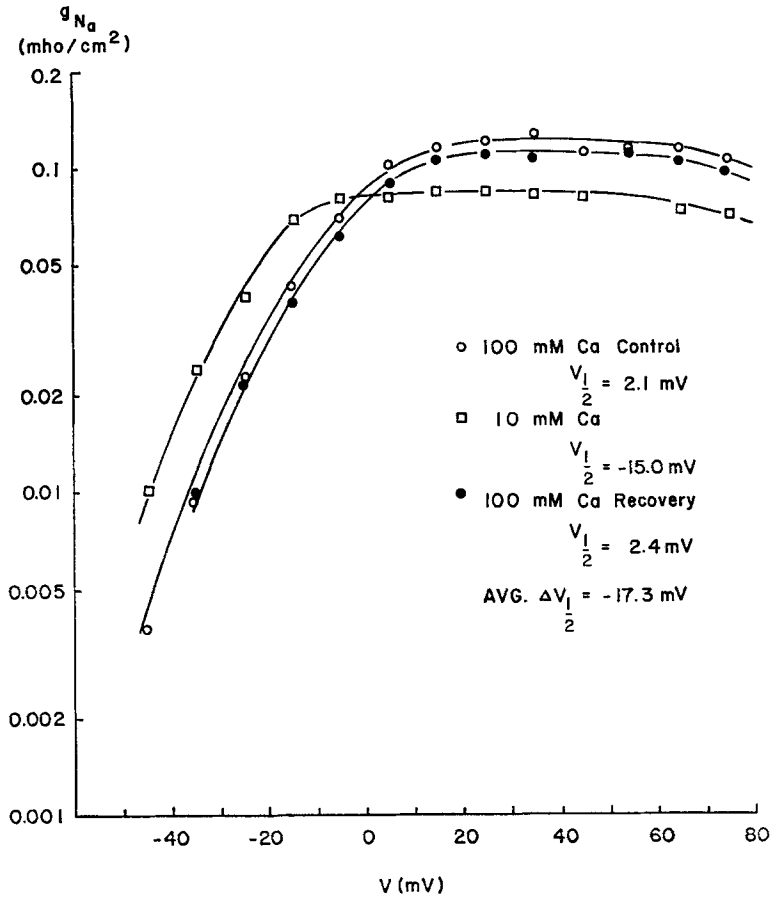

FIGURE 1. Na conductance and Ca. g_{Na} in 100 Ca ASW control solution (open circles), 10 Ca ASW (open squares), and recovery in 100 Ca ASW (filled circles). Solid lines are only for visual reference. $V_{1/2}$ values for the various solutions are indicated.

Ca^{++} control value, $\Delta V_{1/2}$, is used as a measure of the surface potential change.

The apparent reduction of maximum g_{Na} in the low Ca^{++} solution is probably a result of long-term inactivation, described by Adelman and Palti (1969). In this solution the potential within the membrane, as opposed to that between the voltage electrodes, is some 17 mV depolarized from the value in 100 mM Ca^{++}. This long-term inactivation cannot be removed by the relatively short (90 ms) hyperpolarizing prepulse used in my experiments. In one experiment, the membrane potential was held 20 mV more hyperpolarized than usual and there was then only a 5% decrease in the maximum g_{Na} in the 10 Ca^{++} solution. The observed average 25% reduction of g_{Na} for the 100–10 mM calcium concentration change is, then, probably explained by the effects of long-term inactivation.

Note that the $V_{1/2}$ value in high Ca^{++} recovers to its original value as well as or better than the recovery of the maximum conductance. This is a consistent finding and it is reassuring to know that the parameter of interest, $V_{1/2}$, is independent of maximum g_{Na}. In five experiments, the value of $V_{1/2}$ recovered to within about 0.5 mV of the original value. In the other experiments, a return to the 100 mM Ca^{++} solution was not made. The $\Delta V_{1/2}$ values reported, then, are sometimes the average of two measurements (i.e., two 100 Ca^{++} solution values).

As pointed out in Methods, there is a residual uncompensated series resistance, R_s, in my experiments. Hodgkin et al. (1952) and Goldman and Schauf (1972) have pointed out some of the possible errors associated with such uncompensated R_s. Therefore, an attempt was made to determine the degree to which uncompensated R_s affects the measured values of $\Delta V_{1/2}$.

In one experiment (axon A-48), a compensation for series resistance of both 5 and 10 Ω-cm² was used and the shift produced by a 20-fold reduction in Ca^{++} in the position of the peak of the I_{Na}-V curve was monitored. Although the peaks occurred at different voltages, the shift of the peak was the same with both 5- and 10-Ω-cm² compensation, indicating little error in $\Delta V_{1/2}$ measurements. In a second experiment (A-49), $\Delta V_{1/2}$ for a 100-25 Ca^{++} ASW solution change was measured twice: once with 5 Ω-cm² of compensation and once with 10 Ω-cm² of compensation. The difference in these two $\Delta V_{1/2}$ values was only 1.5 mV, an error that would not cause any serious changes in the conclusion about surface charge density. The magnitude of the error produced by uncompensated R_s is a function of the membrane current. In the experiment mentioned above in connection with long-term inactivation there was about a 1.5 mA/cm² increase in I_{Na} when the inactivation was removed. This produced only 1.1-mV change in $V_{1/2}$ for the 10 mM Ca^{++} solution so residual uncompensated R_s probably produces less than a 1- to 2-mV error in the measurements of $V_{1/2}$.

TABLE II

SHIFT OF g_{Na} WITH CHANGES IN $[Ca]_o$ RELATIVE TO 100 mM $[Ca]_o$

Axon	[Ca]	$\Delta V_{1/2}$
A-37	5	−19.4
A-40	5	−20.4
A-48	5	−21.0
A-32	10	−15.1
A-36	10	−17.3
A-41	10	−16.7
A-42	10	−16.7
A-43	10	−18.3
A-50	10	−17.1
A-31	25	−13.1
A-32	25	−11.2
A-34	25	−12.0
A-49	25	−12.8
A-37	50	−3.2
A-48	50	−8.5
A-49	50	−9.5
Average	50	−7.1±2.0
± SEM	25	−12.3±0.43
	10	−16.9±0.43
	5	−20.3±0.47

Experiments such as that of Fig. 1 were repeated using various concentrations of Ca^{++} and the results are summarized in Table II. The average values of $\Delta V_{1/2}$ from Table II have been plotted versus the log of the external calcium concentration in Fig. 2 (the open circles plus SEM limits).

The dashed line in Fig. 2 is the best fit from the Grahame equation and represents a surface charge density of one negative electronic charge, e, per 100 A^2, with a calcium binding constant, K, of zero. It is clear that this fit is much better than with $\sigma = -1$ e/120 A^2 or $\sigma = -1$ e/80 A^2 which also appear in this figure and also with $K = 0.0$.

A unique value of σ and K cannot be found from these data, but an upper limit on the binding constant can be found. As shown in Fig. 2 a value of $K = 0.2$ M^{-1} and a surface charge density of -1 e/140 A^2 provides a reasonable fit to the data. The fit is much poorer with any lower charge density, or any larger binding constant. Therefore, there is an upper limit on the surface charge density of -1 e/100 A^2 and a lower limit of -1 e/140 A^2 with a maximum binding constant of 0.2 M^{-1}.

The Grahame equation also predicts changes in surface potential with changes in monovalent cation concentration. Therefore a limited number of

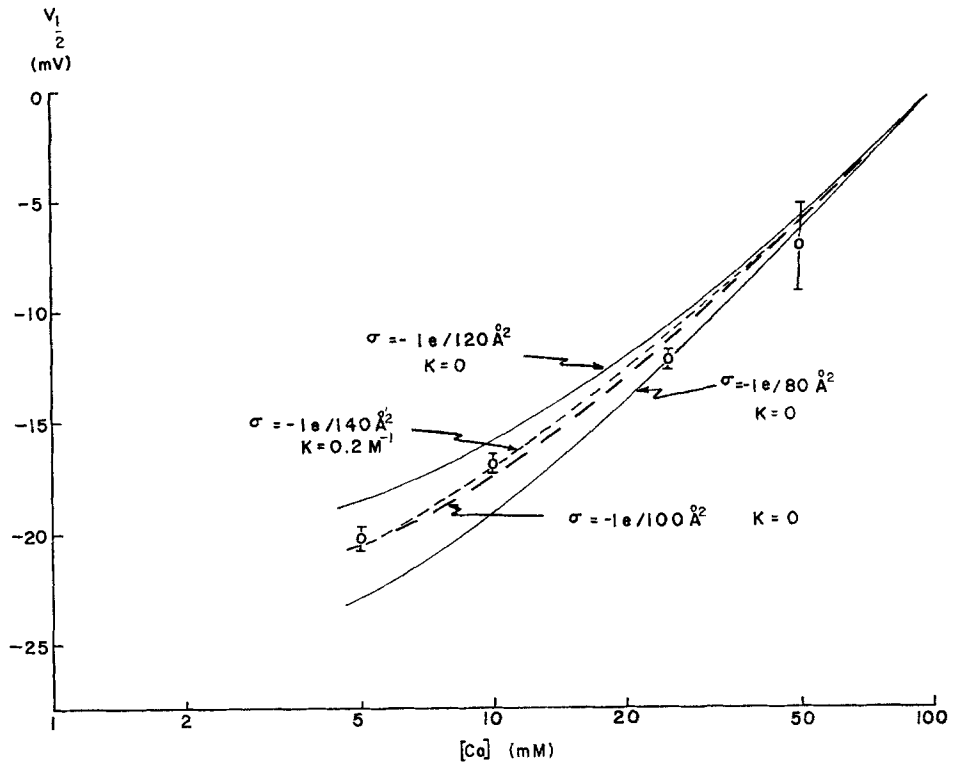

FIGURE 2. $\Delta V_{1/2}$ of g_{Na} and Ca. Open circles are averages (± SEM) of the experimental data. Four theoretical curves (described in text) are drawn and the parameters for each are indicated.

experiments were performed at constant $[Na]_o$ (235 mM), constant $[Ca]_o$ (10 mM), constant $[K]_o$ (10 mM), and three different Tris concentrations (5, 109, and 293 mM, osmolarity maintained with sucrose). The expected shifts from the low Tris solution are 3.7 mV (109 mM) and 9.4 mV (293 mM) for a $\sigma = -1/100$ Å^2, $K = 0$. The measured values of 4.0 ± 0.5 (2) and 8.8 ± 1.7 (3) are consistent with such a surface charge density.

External Calcium and Instantaneous Sodium Current

To see the effects of Ca^{++} on the instantaneous Na currents, I'_{Na}, these currents were measured at two different Ca^{++} concentrations, 10 and 100 mM. This type of experiment is shown in Fig. 3. It should first of all be noted that I'_{Na} values have a linear relationship with V. This is not expected from the constant-field equation which accurately describes instantaneous potassium currents in *Myxicola* axons (Binstock and Goldman, 1971). More importantly, only the slope and not the shape of the I'_{Na} curve changes with the external Ca^{++}. That is, no change in rectification has occurred. The slope was reduced

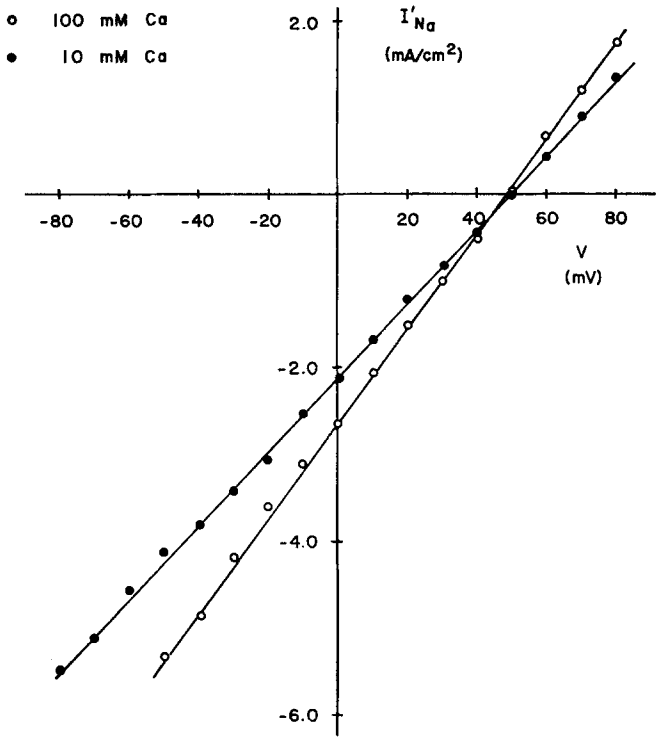

FIGURE 3. Na instantaneous current-voltage relations. Instantaneous Na current-voltage relation in 100 Ca ASW (open circles) and the relation in 10 Ca ASW (filled circles). The lines are straight lines drawn by eye through the data.

by an average factor of 0.16 ± 0.04 for a 100 to 10 Ca^{++} change in three experiments. As indicated above, long-term inactivation probably produces an approximate 25% reduction in sodium conductance for a 100 to 10 mM Ca^{++} change. Taking this into account, the net effect of reducing the calcium concentration from 100 to 10 mM is a slight, perhaps 9%, increase in the slope of the I'_{Na}-V relation.

Fig. 3 demonstrates that there is no effect of external calcium concentration on the shape of the instantaneous sodium current-potential relationship. Both the constant-field equation and the independence relation predict a change in rectification with changes in external sodium concentration. Therefore, to see if the shape did change with external sodium, the experiment of Fig. 4 was performed.

The filled squares in Fig. 4 are the values of I'_{Na} in 25 Ca^{++} ASW, the open squares are I'_{Na} values with half the sodium of the 25 Ca^{++} ASW replaced with Tris. It can be seen that over the range of voltages tested (-50 to $+80$ mV) there is little deviation of either curve from a straight line, drawn by eye through the data points. Identical results were obtained in a second experi-

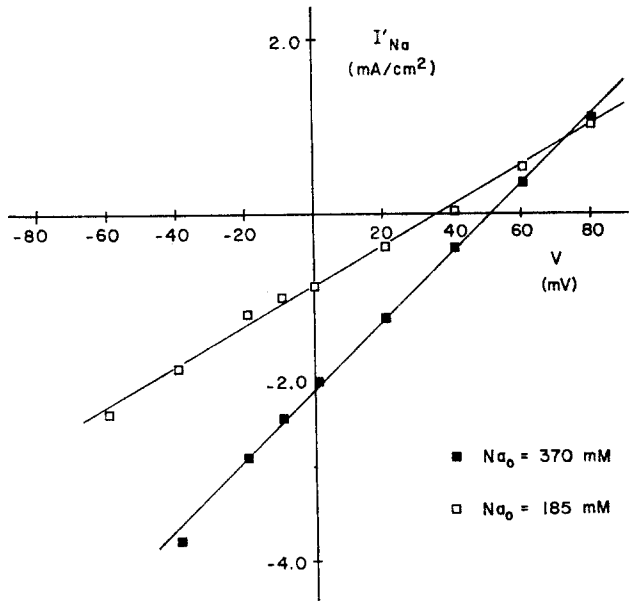

FIGURE 4. Na_o and instantaneous Na currents. Instantaneous Na current, I'_{Na}, as a function of membrane potential, V, in 25 Ca^{++} ASW (filled squares) and in 25 Ca^{++} ASW with half the Na replaced by Tris (open squares).

ment with the same sodium concentrations. At more negative potentials than those shown in this figure, there were deviations from linearity, but this is the range of greatest uncertainty due to the very rapid time-course of the currents. The average reduction in the slope of the lines of the 370 to 185 mM Na change in the two experiments was 0.45 ± 0.03.

In a third experiment with a change of sodium concentration from 370 to 100 mM, similar results were obtained but with greater deviations from linearity in the 100 mM sodium solution. In summary, then, variations in extracellular Ca^{++} produce little alteration of the slope or shape of the I'_{Na}-V relations, while changes in extracellular Na greatly affect the slope, and to a lesser extent the shape, of these relations.

External Calcium and Potassium Conductance

Experiments like those of Fig. 1 were repeated in the presence of TTX to determine the surface charge near the potassium conductance-regulating machinery. Table III summarizes the shifts of g_K at various Ca^{++} concentrations and it is clear that the $\Delta V_{1/2}$ values are more variable and generally quite a bit smaller than the corresponding values for g_{Na} shifts. The best fit to the data is obtained with a negative surface charge density of 1 electronic charge per 325 A^2 with a binding constant of 0.1 M^{-1}. However, reasonable fits are also

TABLE III

SHIFT OF g_K WITH CHANGES IN $[Ca]_o$ RELATIVE TO 100 mM $[Ca]_o$

Axon	$[Ca^{++}]$	$\Delta V_{1/2}$
A-49	50	−1.5
A-48	50	−1.0
A-48	10	−4.0
A-50	10	−7.5
A-46	10	−4.0
A-43	10	−6.5
A-36	10	−12.8
A-44	5	−9.8
A-40	5	−9.3
Average	50	−1.3±0.25
± SEM	10	−7.0±1.6
	5	−9.6±0.25

obtained with a surface charge density as high as −1 e/275 A^2 with no binding and as low as −1 e/350 A^2 with a $K = 0.2\ M^{-1}$.

External Calcium and Instantaneous Potassium Current

Fig. 5 shows two instantaneous potassium current-voltage relations: one in 100 Ca^{++} ASW (open circles) and one in 5 Ca^{++} ASW. The reversal potentials are more positive than the values reported by Binstock and Goldman (1971). The difference may be explained by more loading of the Frankenhaeuser-Hodgkin space (Frankenhaeuser and Hodgkin, 1956) in my experiments. This can result from either a smaller space or more current loading the space (or both). I therefore measured the space thickness in the same manner as Binstock and Goldman (1971) with pulse widths generally of 3–30 ms and found an average value of 2,100 A with a range of 750–4,000 A compared to their values of 2,240 A (range 2,000–3,200 A). Also, my experiments were done at 5°C and theirs at 2°C and g_K increases with temperature. These two observations indicate that the Frankenhaeuser-Hodgkin space in my experiments may have been marginally smaller than that in Binstock and Goldman (1971) and that more current is passed into this smaller space in my experiments. It should be pointed out that this extra loading produces no differences in the interpretation of the results since the instantaneous currents still obey "constant-field" as discussed below.

The reversal potential of the two curves is different by 2.5 mV which is probably due to more loading of the Frankenhaeuser-Hodgkin space in 100 Ca ASW since the currents are larger in this solution. The solid lines in the figures are computed from the constant-field equation using only the respective

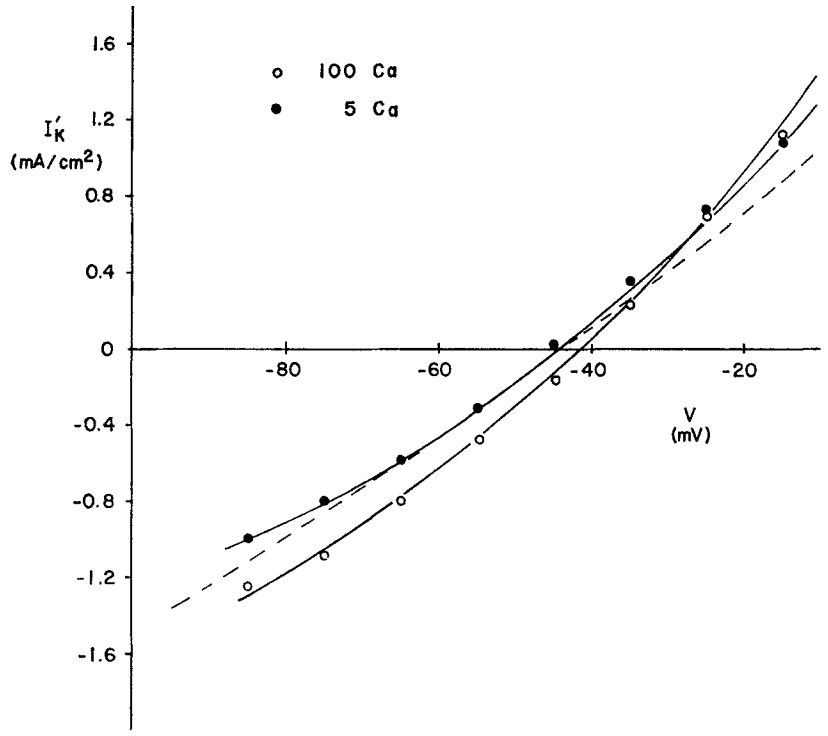

FIGURE 5. Potassium instantaneous current-voltage relations. Potassium instantaneous current, I'_K, as a function of membrane potential, V, in 100 Ca ASW (open circles) and 5 Ca ASW (filled circles). Solid lines are computed from the constant-field equation. Dashed line is computed from the constant-field equation modified to include a surface potential of −35 mV.

reversal potentials and the permeability as a scaling factor. It can be seen that the fit is quite good for both the 100 Ca^{++} and the 10 Ca^{++} data. The smaller currents in 5 Ca ASW in Fig. 5 may be due to an effect of calcium on the magnitude of the permeability or due to the effects of slow inactivation of the potassium conductance (Ehrenstein and Gilbert, 1966). No experiments were done to distinguish between these two possibilities.

As pointed out in the previous section, my observations are consistent with a surface charge density near the potassium voltage sensor of about 1 e/325 A^2 and a binding constant of 0.1 M^{-1}. From Eq. 1 the value of the corresponding surface potential may be calculated and is found to be about −35 mV in 5 Ca ASW. If this surface potential also existed near the potassium pore, then the dashed line of Fig. 5, which is a solution of the constant-field equation modified to include surface potentials (Frankenhaeuser, 1960) should describe the 5 Ca ASW data. It clearly does not, so there is very little surface charge near the potassium pore and certainly no surface charge as large as that near the potassium voltage sensor.

DISCUSSION

Comparison of Results with Published Data

SURFACE CHARGE DENSITY FROM VOLTAGE SHIFTS Frankenhaeuser and Hodgkin (1957), working with squid giant axons, found that a fourfold decrease in external Ca^{++} concentration produced a 12-mV shift of g_{Na}. For an equivalent change in Ca^{++} concentration (100 to 25 mM), I also find a 12-mV shift. They found approximately the same shift of the potassium *slope* conductance, dI_K/dV_m, with external calcium changes, but with less compelling data. Their results indicate a value of about -1 e/120 A^2 for the surface charge density near both sodium and potassium voltage sensors.

Gilbert and Ehrenstein (1969) have reported an average value of $\sigma = -1$ e/120 A^2 and lower limit of -1 e/280 A^2 with a binding constant of 0.1 M^{-1} for the surface charge associated with g_K for the squid giant axon. The difference between the average and the minimum values indicates rather variable results similar to those seen in this study.

I have analyzed Hille's (1968) data on the shifts of g_{Na} in myelinated nerve fibers produced by changes in calcium concentration in the same manner as my own data (cf., Fig. 2) and the data are fitted extremely well with a negative surface charge density of about 1 e/90 A^2 with no binding constant. I did not attempt to see what other surface charge densities could be used in the presence of calcium binding. Hille (1968) shows very little shift of potassium parameters with changes in external calcium.

Recently, Hille et al. (1974) have made a careful analysis of the surface charge associated with the sodium conductance and find an average surface charge density (at pH = 7.4) of -1 e/100 to -1 e/200 A^2 with a binding constant of 0.035–0.83 M^{-1}, respectively.

Brismar (1973) from changes in both monovalent and divalent (Ca^{++}) ion concentrations on frog node, has calculated a surface charge density of about -1 e/290 A^2 associated with g_K (actually potassium permeability, P_K). Although he suggests that this value is also consistent with his data for g_{Na} (P_{Na}), an examination of his results shows that a value closer to -1 e/160 A^2 would be more suitable for the sodium system.

Mozhayeva and Naumov (1970), also working with the frog node, calculated a surface charge density associated with g_K of -1 e/500 A^2 to -1 e/800 A^2 and a binding constant near 5 M^{-1}. However, in their double-layer analysis, they considered only univalent ions and neglected the contribution of divalent cations to the screening process. This omission may account for the low density and the high binding constant.

Table IV summarizes the surface charge densities from the various experiments described above. A rather interesting picture arises from these comparisons: in spite of the rather disparate evolutionary background of vertebrates

TABLE IV
SURFACE CHARGE DENSITIES OF VARIOUS PREPARATIONS

Nerve	g_{Na}		g_K	
	$\sigma(-e/A^2)$	$K(M^{-1})$	$\sigma(-e/A^2)$	$K(M^{-1})$
Squid*	1/120		1/120	
Squid‡			1/120–1/280	0.1
Frog§	1/90	0	small	
Frog″	1/100–1/200	0.035–0.83		
Frog¶			1/500–1/800	5.0
Toad**	1/160	0	1/290	
Worm‡‡	1/100–1/140	0–0.2	1/275–1/350	0.1–0.2

* Frankenhaeuser and Hodgkin (1957); my calculations on their data.
‡ Gilbert and Ehrenstein (1969).
§ Hille (1968), my calculations on his data.
″ Hille et al. (1974).
¶ Mozhayeva and Naumov (1970).
** Brismar (1973), my calculations on his g_{Na} (P_{Na}) data.
‡‡ Begenisich (this paper).

and invertebrates, the surface charge densities associated with the membrane conductances are quite remarkably the same. Although there is some variability, I think it is quite reasonable to conclude that there may generally be a surface charge density near the Na gates on the order of -1 e/140 A^2. The surface charge density near the K gates may be half this value or about -1 e/275 A^2.

It is of some interest to compare these surface charge densities with those found on phospholipid bilayers. McLaughlin et al. (1971) have shown that a negative surface charge density of about 1 e/38 A^2 exists on phospholipid bilayers made from phosphatidylserine or phosphatidylglycerol. This is a considerably higher density than that found from shifts of g_{Na} or g_K as described above.

INSTANTANEOUS POTASSIUM CURREET-VOLTAGE RELATIONS That the instantaneous potassium current-voltage relations in my experiments are described by the constant-field equation is in agreement with the published work of Binstock and Goldman (1971), also on *Myxicola* axons.

There is no published work on the effects of divalent cations on Na or K instantaneous current-voltage relations. However, pH changes also lead to conductance shifts due to alterations of surface potentials in many preparations (Hille, 1968; Woodhull, 1973) including crayfish giant axons (Shrager, 1974). Potassium instantaneous current-voltage relations in crayfish rectify and there is no substantial change in the rectification when the pH is lowered from 7.5 to 5.8 (Shrager, 1974). The same pH change shifts g_K in crayfish by 25 mV (Shrager, 1974). Thus in crayfish axons, as in *Myxicola* axons, g_K can be shifted by screening surface charges with little effect on the rectification of the I'_K-V relation.

INSTANTANEOUS SODIUM CURRENT-VOLTAGE RELATIONS Hodgkin and Huxley (1952) have reported a linear instantaneous sodium I'_{Na}-V in squid giant axons with perhaps a slight deviation from linearity at large negative membrane potentials. In one experiment, they obtained an I'_{Na}-V relation while lowering the external sodium concentration to about 10% of normal and found more significant deviations from linearity. Since they used a much larger sodium concentration change and made their measurements while the solution was still changing, any exact comparison to my data cannot be made. However, there is qualitative agreement in the direction of the deviations from linearity.

Implications of the Results

MEMBRANE POTENTIAL Since the mechanism regulating membrane conductance is voltage sensitive, it is important to know the voltage at this regulating site. My results show that there is a surface potential that affects the operation of the sodium gating mechanism and a calculation from the measured surface charge shows this potential to be about -45 mV (-20 mV near K gates) in normal ASW. This means that when the electrodes measure a zero potential difference, there is actually a potential difference of 45 mV (inside positive) across the membrane containing the conductance-regulating machinery. Furthermore, if there is a positive internal surface potential, the potential across the membrane is even greater. A negative internal surface potential as suggested for squid by Chandler et al. (1965) would lessen the voltage drop. An effort should be made to measure the equivalent internal surface potential of *Myxicola* axons so that the potential "seen" by the voltage sensors can be known.

SPATIAL DISTRIBUTION OF MEMBRANE COMPONENTS: SODIUM AND POTASSIUM VOLTAGE SENSORS The different values for the surface charge near Na and K voltage sensors suggest a spatial separation for these two structures. To arrive at a physical dimension for this separation, it is necessary to consider the dependence of potential on the distance from a charged surface for two cases: a high ionic strength, high dielectric constant medium like an aqueous salt solution, and a low ionic strength, low dielectric constant medium like a lipid.

For a monovalent salt concentration of 500 mM (such as ASW) and a dielectric constant of 80, the distance in which the potential falls to 0.37 of its initial value (the Debye length) is reckoned to be 4.5 A. The case for the lipid medium is not so simple; it is not clear what ionic concentration to use in the calculation. However, certainly any value larger than 1 mM would be too great. With this concentration, then, and using $\epsilon = 6$, the Debye length is found to be 27.5 A.

It is not known whether the voltage sensor controlling conductance is located in the lipid or the electrolytic phase or is part of a protein of intermediate ionic and dielectric strength. Therefore, the above calculation of Debye lengths

should be considered limiting values for voltage sensor separations. If the same charged groups contribute to the effective surface charge of both the Na and K voltage-sensing structures, then these two structures are on the average at least 4.5 A apart if the sensors are in the electrolytic phase, and at least 27.5 A apart if the sensors are in the lipid phase. If, on the other hand, the surface charges near Na and K voltage sensors are separate molecules, the sensors could be much farther apart.

As pointed out above, charged phospholipids have a surface charge density much greater than that near Na and K voltage sensors. Therefore, the Na and K voltage sensors are probably in a region of neutral phospholipids and away from a high density of charged phospholipids. This conclusion pertains also to both the Na and K pores.

SPATIAL DISTRIBUTION OF MEMBRANE COMPONENTS: POTASSIUM VOLTAGE SENSOR AND POTASSIUM PORE There is very little, if any, surface charge near the K pores as indicated by the lack of change of rectification of the potassium instantaneous *I-V* when the external calcium concentration was altered. Also, as shown in Fig. 5, the surface charge near the potassium voltage sensor would, if this charge were also near the pore, produce a curve with far less rectification than is actually seen. Binstock and Goldman (1971) were able to describe the instantaneous potassium *I-V*'s of *Myxicola* axons with the constant-field equation with no need to include surface charge considerations. By arguments such as those of the preceding section, these observations indicate a spatial separation of the K pore and the K voltage sensor. However, it should be noted that the presence of a negative internal surface potential near the K pore would increase the difficulty of resolving a difference in surface charge density between the pore and the voltage sensor.

SPATIAL DISTRIBUTION OF MEMBRANE COMPONENTS: SODIUM VOLTAGE SENSOR AND SODIUM PORE If the sodium pore were near the sodium voltage sensor, a change in external calcium from 10 to 100 mM would, according to the Boltzmann relation, produce a twofold reduction in the local sodium concentration due to the change in the surface potential. Such a reduction in Na concentration should reduce the slope of the I'_{Na}-V relation by about 45% as shown in Fig. 4 for such a Na concentration change. The observed effect, however, was a 16% *increase* in the slope for the 10 to 100 mM Ca^{++} change (Fig. 3). Only two experiments were done with this sodium concentration change and the results from the 10 to 100 mM Ca^{++} change are complicated by the presence of long-term inactivation. However, with these two qualifications, the differential effect on I'_{Na} of changes in calcium and sodium concentration suggests that the voltage sensor is not in the vicinity of the pore which has little surface charge associated with it that is accessible to Ca^{++}.

A similar conclusion was reached by Henderson et al. (1973), based on the fact that calcium ions displace TTX and saxitoxin (STX) from solubilized

garfish olfactory nerves to the same extent, and to almost the same extent from whole nerve. Since STX is doubly charged (and TTX is singly charged) it would be expected that changes in the surface potential produced by changes in calcium concentration would affect STX binding to a much greater degree than TTX binding. They concluded: "Saxitoxin and Tetrodotoxin bind to sodium channels in nerve at a site that is not identical with the region bounding the voltage sensors that regulate channel permeability."

The calculated value of the Debye length in an electrolyte like ASW is small, about the size of a hydrated ion. Therefore, undue significance should not be placed on the amount of separation of the voltage sensors and pores. They are not identical structures, but the degree of separation is uncertain. It is hoped, however, that the use of instantaneous current-voltage relations to investigate the molecular properties of pores will be refined to obtain more definitive results.

MOLECULAR STRUCTURE OF SODIUM AND POTASSIUM PORES Hille (1971, 1972) has proposed an anionic site in the sodium pore of frog node to account for its ionic selectivity. Woodhull (1973) has shown that this site may be one-quarter of the way down the membrane potential. This charged site, then, may be sufficiently within the pore that it cannot be screened by calcium ions, consistent with my results. Furthermore, it may be the presence of this charge which accounts for the observed linear instantaneous current-voltage relations.

Potassium pores exhibit constant-field rectification and might be expected to be relatively free of fixed charges. Hille's (1973) observations on the effects of external pH changes on potassium currents tend to support this view.

The molecular structure of the Na and K pores are therefore likely to be quite different: the Na pore may have a fixed charge site toward the middle of the Na pore and the potassium pore probably contains little fixed charge.

I thank Dr. L. J. Mullins for support and advice throughout all stages of this work. I am indebted to Dr. L. Goldman for many fruitful discussions and to Dr. R. A. Sjodin, Dr. G. Ehrenstein, and Dr. B. Hille for their critical reading of the manuscript.

This research was supported in part by grants from the National Institute of Neurological Diseases and Stroke (NS-05846) and from the National Science Foundation (GB-24585).

Received for publication 27 November 1974.

REFERENCES

ADELMAN, WILLIAM J., JR., and YORAM PALTI. 1969. The effects of external potassium and long duration voltage conditioning on the amplitude of sodium currents in the giant axon of the squid, *Loligo pealei*. *J. Gen. Physiol.* **54**:589.

AVEYARD, R., and D. A. HAYDON. 1973. An introduction to the Principles of Surface Chemistry. Cambridge University Press, New York.

BEGENISICH, T., and C. LYNCH. 1974. Effects of internal divalent cations on voltage-clamped squid axons. *J. Gen. Physiol.* **63**:675.

BINSTOCK, L., and L. GOLDMAN. 1969. Current- and voltage-clamped studies on *Myxicola* giant axons. Effects of tetrodotoxin. *J. Gen. Phsiol.* **54**:730.

BINSTOCK, L., and L. GOLDMAN. 1971. Rectification in instantaneous potassium current-voltage relations in *Myxicola* giant axons. *J. Physiol.* (*Lond.*). **217**:517.

BLAUSTEIN, M. P., and D. E. GOLDMAN. 1968. The action of certain polyvalent cations on the voltage-clamped lobster axon. *J. Gen. Physiol.* **51**:279.

BRISMAR, T. 1973. Effects of ionic concentration on permeability properties of nodal mebrane in myelinated nerve fibres. of *Xenopus laevis*. *Acta Physiol. Scand.* **87**:474.

CHANDLER, W. K., A. L. HODGKIN, and H. MEVES. 1965. The effect of changing the internal solution on sodium inactivation and related phenomena in giant axons. *J. Physiol.* (*Lond.*). **180**:821.

CHANDLER, W. K., and H. MEVES. 1965. Voltage clamp experiments on internally perfused giant axons. *J. Physiol.* (*Lond.*). **180**:788.

COLE, K. S., and J. W. MOORE. 1960. Liquid junction and membrane potentials of the squid giant axon. *J. Gen. Physiol.* **43**:971.

DAVIES, J. T., and E. K. RIDEAL. 1963. Interfacial Phenomena. Academic Press, Inc., New York. 2nd edition.

EHRENSTEIN, G., and D. L. GILBERT. 1966. Slow changes of potassium permeability in the squid giant axon. *Biophys. J.* **6**:553.

FISHMAN, S. N., B. I. KHODOROV, and M. V. VOLKENSTEIN. 1971. Molecular mechanisms of membrane ionic permeability changes. *Biochim. Biophys. Acta.* **225**:1.

FRANKENHAEUSER, B. 1960. Sodium permeability in toad nerve and in squid nerve. *J. Physiol.* (*Lond.*). **152**:159.

FRANKENHAEUSER, B., and A. L. HODGKIN. 1956. The aftereffects of impulses in the giant nerve fibres of *Loligo*. *J. Physiol.* (*Lond.*). **131**:341.

FRANKENHAEUSER, B., and A. L. HODGKIN. 1957. The action of calcium on the electrical properties of squid axons. *J. Physiol.* (*Lond.*). **137**:218.

GILBERT, D. L., and G. EHRENSTEIN. 1969. Effect of divalent cations on potassium conductance of squid axons: Determination of surface charge. *Biophys. J.* **9**:447.

GOLDMAN, D. E. 1964. A molecular structural basis for the excitation properties of axons. *Biophys. J.* **4**:167.

GOLDMAN, L., and C. L. SCHAUF. 1972. Inactivation of the sodium current in *Myxicola* axons. Evidence for coupling to the activation process. *J. Gen. Physiol.* **59**:659.

GRAHAME, D. C. 1947. The electrical double layer and the theory of electrocapillarity. *Chem. Rev.* **41**:441.

HENDERSON, R., J. M. RITCHIE, and G. R. STRICHARTZ. 1973. The binding of labelled saxitoxin to the sodium channels in nerve membranes. *J. Physiol.* (*Lond.*). **235**:783.

HILLE, B. 1968. Charges and potentials at the nerve surface. Divalent ions and pH. *J. Gen. Physiol.* **51**:221.

HILLE, B. 1971. The permeability of the sodium channel to organic cations in myelinated nerve. *J. Gen. Physiol.* **58**:599.

HILLE, B. 1972. The permeability of the sodium channel to metal cations in myelinated nerve. *J. Gen. Physiol.* **59**:637.

HILLE, B. 1973. Potassium channel in myelinated nerve. Selective permeability to small cations. *J. Gen. Physiol.* **61**:669.

HILLE, B., A. WOODHULL, and B. SHAPIRO. 1975. Negative surface charge near sodium channels of nerve: Divalent ions, monovalent ions, and pH. *Philos. Trans. R. Soc. Lond. B. Biol. Sci.* In press.

HODGKIN, A. L., and A. F. HUXLEY. 1952. The components of membrane conductance in the giant axon of *Loligo*. *J. Physiol.* (*Lond.*). **116**:473.

HODGKIN, A. L., A. F. HUXLEY, and B. KATZ. 1952. Measurement of current-voltage relations in the membrane of the giant axon of *Loligo*. *J. Physiol.* (*Lond.*). **116**:424.

MCLAUGHLIN, S. G. A., G. SZABO, and G. EISENMAN. 1971. Divalent ions and the surface potential of charged phospholipid membranes. *J. Gen. Physiol.* **58**:667.

MOORE, L. E., and E. JAKOBSSON. 1971. Interpretation of the sodium permeability changes of myelinated nerve in terms of linear relaxation theory. *J. Theor. Biol.* **33**:77.

MOZHAYEVA, G. N., and A. P. NAUMOV. 1970. Effect of surface charge on the steady-state potassium conductance of nodal membrane. *Nature* (*Lond.*). **228**:164.

ROJAS, E., and I. ATWATER. 1968. An experimental approach to determine membrane charges in squid giant axons. *J. Gen. Physiol.* **51**:(5, Pt. 2):131s.

SHRAGER, PETER. 1974. Ionic conductance changes in voltage clamped crayfish axons at low pH. *J. Gen. Physiol.* **64**:666.

WOODHULL, ANN M. 1973. Ionic blockage of sodium channels in nerve. *J. Gen. Physiol.* **61**:687.